

# On the stability of Hopfions in the two-component Ginzburg-Landau model

J. Jäykkä\* and J. Hietarinta†

*Department of Physics, University of Turku, FI-20014 Turku, Finland*

P. Salo‡

*Laboratory of Physics, Helsinki University of Technology,  
P.O. Box 1100, FI-02015 TKK, Espoo, Finland*

(Dated: May 4, 2019)

We study the stability of Hopfions embedded in the Ginzburg-Landau model of two oppositely charged components. It has been shown by Babaev *et al.* [Phys. Rev. B **65**, 100512 (2002)] that this model contains the Faddeev-Skyrme model, which is known to have topologically stable configurations with a given Hopf charge. The Ginzburg-Landau model, however, contains extra fields and this can in principle change the fate of topologically non-trivial configurations. We investigate the stability of Hopfions in this model both analytically (scaling) and numerically (first order dissipative dynamics). A number of initial states with different Hopf charges are studied, and we also consider potentials with different singularities.

PACS numbers: 74.20.De, 47.32.cd

## I. INTRODUCTION

Topologically stable knots and other vortex-like structures have recently received wide interest within condensed matter physics. One reason for this is the continuous development of experimental techniques which now allow the production of vortices in various types of media. These include, e.g., Bose-Einstein condensates<sup>1,2</sup>, superconductors<sup>3,4,5</sup>, superfluid <sup>3</sup>He<sup>6,7</sup> and nematic liquid crystals<sup>8</sup>. At the same time the increased capacity of supercomputers has made it possible to study these structures numerically. Thus, in the last decade there have been many numerical studies devoted to finding stable topologically non-trivial configurations in different physical systems, this includes, e.g., topological unknotted, knots and vortices in the Faddeev-Skyrme (FS) model<sup>9,10,11,12,13,14,15</sup>, vortices in Bose-Einstein condensates<sup>16,17,18</sup>, vortex atom lasers in a two-flavor Bose condensate<sup>19</sup> and vortices in superconductors<sup>20,21</sup>, liquid helium<sup>22,23</sup>, liquid metallic hydrogen<sup>24</sup> and possibly even in neutron stars<sup>25</sup>.

There are various ways in which a vector field in material can support vortices. For example the velocity field can form a vortex, e.g., in a hurricane. The position of the vortex is in the eye of the hurricane, where the velocity is zero. Such a vortex is not stable, because a velocity field can continuously change to zero everywhere.

In some special materials there can exist vector fields, associated to spin or other such property, that cannot vanish. Then it is possible to have vortices that are both non-singular and conserved, the conservation following from topological reasons. (One example is the continuous unlocked vortex (CUV) in superfluid <sup>3</sup>He-A<sup>6</sup>.) The prototype model that contains non-vanishing topological structures characterized by a Hopf charge was presented by L. Faddeev<sup>9,26</sup>, and recently it has been shown numerically that this model does indeed contain stable topological solitons<sup>10,11,12,13</sup>.

In this work we study numerically a system of two electromagnetically coupled, oppositely charged Bose condensates described by the Ginzburg-Landau (GL) model. Babaev *et al.* studied this system in Ref.<sup>27</sup> and argued that it should contain stable knotted vortex solitons with non-zero Hopf charge. Here we present our results for the simulations of the GL model and discuss the terms under which this model could have topologically stable solutions. The paper is organized as follows: In Section II we formulate the equations, discuss the possible potentials and present the initial states that are used in the computation. In Section III we present the numerical method of finding stable minimum energy configurations. In Section IV we describe the results and finally in Section V we give some concluding remarks on the results obtained.

## II. MODEL

### A. Ginzburg-Landau model

The model describes two electromagnetically coupled, oppositely charged Bose condensates, as given by the GL Lagrangian density

$$\mathcal{L} = \frac{\hbar^2}{2m_1} \left| (\nabla + i\frac{2e}{\hbar c}\vec{A})\Psi_1 \right|^2 + \frac{\hbar^2}{2m_2} \left| (\nabla - i\frac{2e}{\hbar c}\vec{A})\Psi_2 \right|^2 + V(\Psi_1, \Psi_2) + \frac{1}{2\mu_0} \vec{B}^2, \quad (1)$$

where we have used SI units. In Eq. (1)  $\Psi_1$  and  $\Psi_2$  are the order parameters for the condensates,  $\vec{A}$  is the electromagnetic vector potential,  $\vec{B}$  the magnetic field,  $\vec{B} = \frac{1}{c}\nabla \times \vec{A}$ , and  $V$  is a potential.

Babaev *et al.*<sup>27</sup> introduced new variables by setting

$$\Psi_k = \sqrt{2m_k\rho}\chi_k, \quad (2)$$

where the new complex field  $\chi$  is normalized as

$$|\chi_1|^2 + |\chi_2|^2 = 1, \quad (3)$$

and therefore the real field  $\rho$  is given by

$$\rho^2 = \frac{1}{2} \left( \frac{|\Psi_1|^2}{m_1} + \frac{|\Psi_2|^2}{m_2} \right). \quad (4)$$

In terms of the new fields of (2) Eq. (1) becomes

$$\begin{aligned} \mathcal{L} = & \hbar^2 \rho^2 \left( \left| \left( \nabla + i \frac{2e}{\hbar c} \vec{A} \right) \chi_1 \right|^2 + \left| \left( \nabla - i \frac{2e}{\hbar c} \vec{A} \right) \chi_2 \right|^2 \right) \\ & + \hbar^2 (\nabla \rho)^2 + V(\chi_1, \chi_2, \rho^2) + \frac{1}{2\mu_0} \vec{B}^2. \end{aligned} \quad (5)$$

The Lagrangian (1) is invariant under the gauge transformation

$$\begin{cases} \Psi_1 & \rightarrow e^{-i \frac{2e}{\hbar} \theta(x)} \Psi_1 \\ \Psi_2 & \rightarrow e^{i \frac{2e}{\hbar} \theta(x)} \Psi_2 \\ A_\mu & \rightarrow A_\mu + c \partial_\mu \theta(x), \end{cases} \quad (6)$$

and the corresponding Nöther current is

$$\begin{aligned} J_k = & \frac{i\hbar e}{m_1} (\Psi_1^* \partial_k \Psi_1 - \Psi_1 \partial_k \Psi_1^*) - \frac{i\hbar e}{m_2} (\Psi_2^* \partial_k \Psi_2 - \Psi_2 \partial_k \Psi_2^*) \\ & - \frac{4e^2}{c} \left( \frac{|\Psi_1|^2}{m_1} + \frac{|\Psi_2|^2}{m_2} \right) A_k. \end{aligned} \quad (7)$$

When we use the new variables (2) here, we obtain

$$\begin{aligned} J_k = & 2e\hbar\rho^2 i (\chi_1^* \partial_k \chi_1 - \chi_1 \partial_k \chi_1^* - \chi_2^* \partial_k \chi_2 + \chi_2 \partial_k \chi_2^*) \\ & - \frac{8e^2 \rho^2}{c} A_k \\ = & 4e\hbar\rho^2 \left( \frac{1}{2} j_k - \frac{2e}{\hbar c} A_k \right), \end{aligned} \quad (8)$$

which contains a new (non-gauge invariant) current<sup>28</sup>

$$j_k = i (\chi_1^* \partial_k \chi_1 - \chi_1 \partial_k \chi_1^* - \chi_2^* \partial_k \chi_2 + \chi_2 \partial_k \chi_2^*). \quad (9)$$

Later on we also use a gauge invariant vector

$$\vec{C} = \frac{1}{\hbar e \rho^2} \vec{J}. \quad (10)$$

Next we define the unit vector field  $\vec{n}$  by

$$\vec{n}^T = (\chi_1^* \ \chi_2) \vec{\sigma} \begin{pmatrix} \chi_1 \\ \chi_2^* \end{pmatrix} = \begin{pmatrix} \chi_1 \chi_2 + \chi_1^* \chi_2^* \\ i(\chi_1 \chi_2 - \chi_1^* \chi_2^*) \\ |\chi_1|^2 - |\chi_2|^2 \end{pmatrix}, \quad (11)$$

where  $\vec{\sigma}$  are the Pauli matrices. The inverse transformation is

$$\begin{cases} \chi_1 = \frac{n_1 - i n_2}{\sqrt{2(1-n_3)}} e^{i\alpha}, \\ \chi_2 = \frac{\sqrt{1-n_3}}{\sqrt{2}} e^{-i\alpha}, \end{cases} \quad (12)$$

where the phase  $\alpha$  cannot be determined from  $\vec{n}$ .

The aim is now to write the Lagrangian (5) in terms of  $\vec{n}$ ,  $\rho$  and  $\vec{C}$ , after which the  $\vec{n}$  part of the result should be similar to the FS model, given by

$$\mathcal{L}_{\text{FS}} = \frac{1}{2} \partial_k n_l \partial^k n^l + g_{\text{FS}} (\vec{n} \cdot \partial_l \vec{n} \times \partial_m \vec{n})^2. \quad (13)$$

After inverting Eqs. (8) and (10) to obtain  $\vec{A}$  in terms of  $\vec{C}$  and  $\vec{j}$  the kinetic part of Eq. (5) becomes

$$\begin{aligned} \mathcal{L}_{\text{kinetic}} = & \hbar^2 \rho^2 (|\nabla \chi_1|^2 + |\nabla \chi_2|^2 - \frac{1}{4} \vec{j}^2) \\ & + \hbar^2 (\nabla \rho)^2 + \frac{\hbar^2 \rho^2}{16} \vec{C}^2. \end{aligned} \quad (14)$$

Using Eqs. (11), (3) and (9) one finds that

$$\partial_k n_l \partial^k n^l = 4(|\nabla \chi_1|^2 + |\nabla \chi_2|^2) - \vec{j}^2 \quad (15)$$

and therefore the first term in Eq. (14) corresponds to the first term in Eq. (13).

By direct substitution of Eqs. (8) and (10), we also find that

$$\vec{B} = \frac{1}{c} \nabla \times \vec{A} = \frac{\hbar}{4e} (\nabla \times \vec{j} - \frac{1}{2} \nabla \times \vec{C}), \quad (16)$$

and again using Eqs. (11), (3) and (9), we get

$$\frac{1}{2} \epsilon_{klm} \vec{n} \cdot \partial_l \vec{n} \times \partial_m \vec{n} = -(\nabla \times \vec{j})_k, \quad (17)$$

from which we can see that the  $\vec{B}^2$  term in Eq. (5) contributes to the second term in Eq. (13).

Combining the above results we can write the Lagrangian (1) in the form

$$\begin{aligned} \mathcal{L} = & \frac{\hbar^2 \rho^2}{4} \partial_k n_l \partial^k n^l + \hbar^2 (\nabla \rho)^2 + \frac{\hbar^2 \rho^2}{16} \vec{C}^2 + V(\rho, n_i) \\ & + \frac{\hbar^2}{128 \mu_0 e^2} [\epsilon_{ijk} (\vec{n} \cdot \partial_j \vec{n} \times \partial_k \vec{n} + \partial_j C_k)]^2, \end{aligned} \quad (18)$$

which is the form derived by Babaev *et al.*<sup>27</sup>. The dynamical fields are now  $\rho$ ,  $\vec{n}$  and  $\vec{C}$ . If  $\rho = \text{constant}$  and  $\vec{C} = 0$ , the GL model reduces to the FS model in Eq. (13). Since the FS model contains stable topological structures with non-trivial Hopf charge, one can hope that the GL model also contains similar kind of structures. However, GL contains the additional fields  $\rho$  and  $\vec{C}$  in comparison to FS and the role of these new fields must be investigated.

## B. Form of the potential

A typical and rather general quartic potential used in the GL model is

$$\begin{aligned} V_0(\Psi_1, \Psi_2) = & \frac{1}{2} c_1 |\Psi_1|^4 + \frac{1}{2} c_2 |\Psi_2|^4 + c_3 |\Psi_1|^2 |\Psi_2|^2 \\ & + b_1 |\Psi_1|^2 + b_2 |\Psi_2|^2 + a_0. \end{aligned} \quad (19)$$

When  $\Psi$ 's are expressed in terms of  $\rho$  and  $\vec{n}$  and the whole system is rescaled so that  $m_i \rightarrow 1$ , we find

$$|\Psi_1|^2 = \rho^2 (1 + n_3), \quad |\Psi_2|^2 = \rho^2 (1 - n_3), \quad (20)$$

and then the potential (19) reads

$$\begin{aligned} V_0(\rho^2, n_3) = & \rho^4 [n_3^2 (\frac{1}{2}(c_1 + c_2) - c_3) + n_3 (c_1 - c_2) \\ & + \frac{1}{2}(c_1 + c_2) + c_3] \\ & + \rho^2 [n_3 (b_1 - b_2) + b_1 + b_2] + a_0. \end{aligned} \quad (21)$$

One important aspect in choosing the potential is that at infinity the fields will settle to the minimum of the potential. Furthermore, in order to define the Hopf charge it is necessary that the  $\vec{n}$  field points to the same direction far away, otherwise we cannot compactify the 3D-space. It would therefore be optimal to have a potential with a minimum that would fix the  $\vec{n}$  field completely, say, to  $n_3 = 1$ . This may not happen for physically interesting potentials.

For a particular example assume that  $c := c_1 = c_2 = c_3 > 0$ ,  $b := b_1 = b_2$ , then  $n_3$  disappears from Eq. (21) and the potential minimum is at  $\rho^2 = -b/(2c)$ ,  $\vec{n}$  being free. For more generic parameter values the extrema are obtained for particular values of  $n_3$  and  $\rho^2$ :

$$n_3 = \frac{b_1(c_2 + c_3) - b_2(c_1 + c_3)}{b_1(c_2 - c_3) + b_2(c_1 - c_3)}, \quad (22)$$

$$\rho^2 = -\frac{b_1(c_2 - c_3) + b_2(c_1 - c_3)}{2(c_1c_2 - c_3^2)}. \quad (23)$$

This is a minimum, if  $c_1c_2 > c_3^2$ . Note that the above values do not necessarily fall within the allowed values for  $\rho^2$  and  $n_3$ , (i.e.,  $\rho^2 > 0$  and  $|n_3| \leq 1$ ), in which case the extrema are on the boundaries of the allowed values.

From physical arguments the following special case is relevant<sup>29</sup>

$$V_1(\Psi_1, \Psi_2) = \lambda \left( (|\Psi_1|^2 - 1)^2 + (|\Psi_2|^2 - 1)^2 \right), \quad (24)$$

it breaks  $O(3)$  to  $O(2)$  and corresponds to two independently conserved condensates. It has a minimum at  $n_3 = 0$ ,  $\rho^2 = 1$ . Another physically relevant<sup>29</sup> potential is

$$V_2(\Psi_1, \Psi_2) = \lambda \left( (|\Psi_1|^2 - 1)^2 + (|\Psi_2|^2 - 1)^2 \right) + c |\Psi_1 \Psi_2^* - \Psi_2 \Psi_1^*| + a_0, \quad (25)$$

which breaks  $O(3)$  completely. This corresponds to multiband superconductors with interband Josephson effect<sup>29</sup>. In terms of  $\vec{n}$  this potential is given (using Eq. (12))

$$V_2 = \lambda \frac{1}{2} n_3^2 + c \Im[(n_2 - i n_1) e^{i2\alpha}] + a_0. \quad (26)$$

The minimum of this potential is located at  $\rho^2 = 1/2$ ,  $n_3 = \sqrt{1 - c^2/\lambda^2}$ , while the specific values of  $n_1$  and  $n_2$  also depend on  $\alpha$ , which is related to the phase of  $\Psi$ .

From the point of view of Hopf-charge conservation the possibility of  $\rho = 0$  is problematic, even if this happens locally, because then the  $\vec{n}$  field is not defined. However, it has been argued<sup>30</sup> that quantum effects ensure that  $\rho \neq 0$  everywhere. In classical field theories, like the present one, such expected quantum effects can be included through effective potentials. Since the main purpose of this effective potential is to guarantee that  $\rho \neq 0$ , its exact form is not so important. In our computations

we use

$$V_{\text{eff}}(\Psi_1, \Psi_2) = \frac{1}{4} \lambda (|\Psi_1|^2 + |\Psi_2|^2 - \rho_0^2)^2 + 2\gamma (|\Psi_1|^2 + |\Psi_2|^2)^{-1} + a_0. \quad (27)$$

The constants  $\rho_0$  and  $a_0$  are determined by requiring that the minimum of the potential is at  $\rho^2 = 1$  with a value of 0, yielding  $\rho_0^2 = \frac{\gamma}{\lambda} - 2$  and  $a_0 = -\gamma - \frac{\gamma^2}{4\lambda}$ .

### C. Initial states of Hopf invariant Q

We are interested in the minimum energy configurations of topologically distinct configurations of the vector field  $\vec{n}$ , related to the complex physical fields  $\Psi_i$  through Eqs. (2) and (12). From the point of view of  $\vec{n}$  it is only necessary that  $\lim_{|\vec{x}| \rightarrow \infty} \vec{n} = \vec{n}_\infty$  is the same in all directions. From this it follows that we can compactify  $\mathbb{R}^3 \rightarrow \mathbb{S}^3$  and then  $\vec{n}$  becomes a map  $\mathbb{S}^3 \rightarrow \mathbb{S}^2$  with homotopy group  $\pi_3(\mathbb{S}^2) = \mathbb{Z}$ , characterized by the Hopf charge.

Therefore, we have to create a configuration with  $\Psi : \mathbb{R}^3 \rightarrow \mathbb{C}^2$  and  $\vec{A} : \mathbb{R}^3 \rightarrow \mathbb{R}^3$ , such that  $\vec{n}$  has the desired property mentioned above. For  $\Psi_i$  this implies  $|\Psi_1|^2 + |\Psi_2|^2 \neq 0$  and  $\lim_{|\vec{x}| \rightarrow \infty} \Psi_i = \text{constant}$ . The first condition is also necessary for defining the field  $\chi$  and if the second condition is also satisfied  $\chi$  becomes a map  $\mathbb{S}^3 \rightarrow \mathbb{S}^3$ .

The method of constructing a configuration with a desired Hopf charge has been solved by Aratyn *et al.*<sup>31</sup>. The idea is to use the combination of any map  $\phi : \mathbb{S}^3 \rightarrow \mathbb{S}^3$  with the Hopf map  $h : \mathbb{S}^3 \rightarrow \mathbb{S}^2$

$$h(\phi_1, \phi_2, \phi_3, \phi_4) = \begin{pmatrix} 2(\phi_1\phi_3 - \phi_2\phi_4) \\ -2(\phi_1\phi_4 + \phi_2\phi_3) \\ \phi_1^2 + \phi_2^2 - \phi_3^2 - \phi_4^2 \end{pmatrix} \quad (28)$$

to give  $h \circ \phi : \mathbb{S}^3 \rightarrow \mathbb{S}^2$ . We see immediately that if we identify  $\phi_i = \chi_i$ , we have  $\vec{n} = h \circ \phi$ .

For an explicit construction one uses the toroidal coordinates  $(\eta, \xi, \varphi)$  of  $\mathbb{R}^3$  defined by

$$\begin{aligned} x_1 &= \frac{\sinh(\eta) \cos(\varphi)}{q}, & x_2 &= \frac{\sinh(\eta) \sin(\varphi)}{q}, \\ x_3 &= \frac{\sin(\xi)}{q} & q &= \cosh(\eta) - \cos(\xi). \end{aligned} \quad (29)$$

Next take any monotonic function  $g : [0, \infty) \rightarrow [-1, 1]$  and define the map  $\phi : \mathbb{S}^3 \rightarrow \mathbb{S}^3$  by

$$\phi = (g(\eta) \cos(m\xi), g(\eta) \sin(m\xi), \sqrt{1 - g(\eta)^2} \cos(n\varphi), \sqrt{1 - g(\eta)^2} \sin(n\varphi)). \quad (30)$$

If furthermore  $g$  is such that  $\lim_{\eta \rightarrow \infty} g^2(\eta) - \lim_{\eta \rightarrow 0} g^2(\eta) = 1$ , then the combined map,  $h \circ \phi$ , has the Hopf invariant

$$H(h \circ \phi) = nm. \quad (31)$$

For details, see Ref.<sup>31</sup>.

Using Eqs. (11) and (30) and identifying  $\phi_1 + i\phi_2 = \chi_1$  and  $\phi_3 + i\phi_4 = \chi_2$ , we obtain the following form for  $\vec{n}$

$$\vec{n}(x)^T = \begin{pmatrix} 2g(\eta) \sqrt{1-g^2} \cos(m\xi + n\varphi) \\ -2g(\eta) \sqrt{1-g^2} \sin(m\xi + n\varphi) \\ 2g^2(\eta) - 1 \end{pmatrix}. \quad (32)$$

Note that the value of  $\vec{n}_\infty := \lim_{|\vec{x}| \rightarrow \infty} \vec{n}$  (or, equivalently,  $\Psi_\infty := \lim_{|\vec{x}| \rightarrow \infty} \Psi$ ) can be arbitrary, but in order to obtain a finite energy we must have  $V(\Psi_\infty) = 0$ .

We use Eq. (30), expressed in cartesian coordinates, and Eq. (2) to obtain the initial configurations of  $\Psi_i$  for our numerical computations. It is worth noting that these equations are not enough to determine the value of  $\rho^2$ , but the choice of potential which dictates the value of  $\lim_{|\vec{x}| \rightarrow \infty} \Psi_i$  above, simultaneously fixes the *preferred* value of  $\rho^2$ . We use this preferred value for all  $\vec{x}$  when constructing the initial configurations.

It is perhaps useful to mention once more that the change of variables in Eqs. (2)–(4) is not reversible whenever  $\rho(\vec{x}) = 0$ . There is, however, no guarantee that  $\rho$  stays non-zero in numerical simulations of the physical fields  $\Psi_i$  and  $\vec{A}$ , even if the minimum of the potential is at a non-zero value of  $\rho$ . The situation when  $\rho = 0$  locally can imply breakdown in topology and therefore in our numerical simulations we have to follow the changes in the global minimum value of  $\rho$ . It is also worth mentioning that, as we will see later, the discrete nature of a lattice simulation only approximates a continuous deformation and therefore it may occur that the approximation is not good enough, allowing a jump from one homotopy class to another.

### III. NUMERICS

In this section we will describe the discretization of the model and the method of the minimization of the Lagrangian (1). We will also compare the GL to FS model and present some test calculations and the parameters as well as coupling constants for the simulations.

The time-independent, ordinary Abelian  $\mathbb{U}(1)$  Higgs model

$$\mathcal{L} = \frac{1}{2} \left| (\hbar \nabla + ig' \vec{A}) \Psi \right|^2 + V(|\Psi|^2) + \frac{1}{2} g'_F F_{jk}^2 \quad (33)$$

has long since been discretized by lattice field theorists (for example, see Ref.<sup>32,33</sup> and references therein). This is identical to one-component GL theory in an external electromagnetic field and can be immediately applied to our two-component model, where the  $\Psi$  fields are only coupled through the potential  $V$ . The discretization of the electromagnetic vector field  $\vec{A}$  has been done in the canonical way of Ref.<sup>32</sup>. The discretization of the  $\Psi_i$  fields has been done as for the unit vector field  $\vec{n}$  in Ref.<sup>12</sup>. The system has been discretized on a rectangular lattice, with cubic grids of sizes of  $120^3 \dots 960^3$ . Of these just the

sizes  $240^3$ ,  $480^3$  and  $720^3$  were used in actual simulations, the remaining sizes were used only to verify the code, results and discretization.

The minimization of the Lagrangian has been done using the steepest descent method. The gradients needed have been calculated symbolically from the discretized Lagrangian.

For simplicity we have used the rescaled ( $|\Psi_i|^2/m_i \rightarrow |\Psi_i|^2$ ) Lagrangian and natural units ( $c = \hbar = 1$ ) throughout our numerical work. With these choices, the Lagrangian density used in all our numerical simulations becomes

$$\mathcal{L} = \frac{1}{2} \left| (\nabla + ig\vec{A}) \Psi'_1 \right|^2 + \frac{1}{2} \left| (\nabla - ig\vec{A}) \Psi'_2 \right|^2 + \frac{1}{2} g_f (\nabla \times \vec{A})^2 + V_j(\Psi'_{1,2}). \quad (34)$$

This can be further scaled by  $\vec{A} \rightarrow g\vec{A}$ , which reveals the fact that the only relevant parameter is  $g^2/g_f = 4\mu_0 e^2$ . The values used in numerical simulations are  $g = 1$  and  $g_f = 2$ , which amounts to a particular choice of units for  $\mu_0$  and  $e$ .

In order to start the simulations we have to generate initial states with specified Hopf invariants. These initial configurations have been made using Eq. (30) and choosing  $\rho$  such that  $V(\Psi_\infty) = 0$ . As a test of discretization we used the same initial configuration in grids of different sizes and with different lattice constants. With grid sizes of  $240^3$  and above the energies were within 1% of each other.

We have also compared the new calculations with those presented in Ref.<sup>13</sup>. By using an initial configuration, where  $\rho \equiv 1$ ,  $\vec{C} \equiv 0$  and  $V \equiv 0$ , the GL model (18) reduces to the FS model (13). In particular, the magnetic term becomes  $E_{MB} = \frac{\hbar^2}{128\mu_0 e^2} [\epsilon_{ijk} (\vec{n} \cdot \partial_j \vec{n} \times \partial_k \vec{n})]^2$ , while in the FS model we have  $E_{TFS} = \frac{1}{2} g_{FS} (\vec{n} \cdot \partial_l \vec{n} \times \partial_m \vec{n})^2$ . If we set  $2e/c = 1$ ,  $c = \hbar = 1$ ,  $\mu_0 = 1/2$  and  $g_{FS} = 1/8$  (the value most commonly used in the earlier work), we have  $E_{TFS} = E_{MB}$ . (The condition  $\vec{C} = 0$  can be arranged by giving the gauge field  $A_\mu$  a suitable value and the rest of the conditions are simply choices for some units and the constant  $g_{FS}$ , including  $e = 1/2$  and  $\mu_0 = 1$ .) We created the same initial configuration with our old and new codes and found that the energies of the initial states agree to within 1% with a grid of  $120^3$ .

In our previous studies we have always assumed that  $\lim_{|\vec{x}| \rightarrow \infty} n_3 = 1$ , but some of the present potentials, e.g.,  $V_1$ , do not have that as a minimum. In this case we may assume that  $\lim_{|\vec{x}| \rightarrow \infty} n_2 = 1$ , but this can be transformed to  $n_3 = 1$  by a global rotation in the configuration space, which takes  $n_3 \rightarrow n_2$  and  $n_2 \rightarrow -n_3$ . The same effect can be achieved by using new fields defined by

$$\Psi'_1 = \frac{1}{\sqrt{2}} (\Psi_1 + i\Psi_2^*), \quad \Psi'_2 = \frac{1}{\sqrt{2}} (\Psi_2 - i\Psi_1^*). \quad (35)$$

Substituting (35) into (24) gives us a potential which is physically equivalent to  $V_1$ .

During the calculations we have been monitoring the topology of the system. As we saw in Sec. II B, the conservation of topology is not guaranteed whenever  $\rho \rightarrow 0$ . Therefore we have followed the value of the global minimum of  $\rho^2$ . In keeping with our earlier work, we have also been monitoring the dot products of  $\vec{n}(\vec{x}) \cdot \vec{n}(\vec{x} + \vec{\mu})$ , (where  $\vec{\mu} \in \{(1, 0, 0), (0, 1, 0), (0, 0, 1)\}$ ). When the global minimum of this dot product approaches zero or becomes even negative it indicates possible breakdown of topology during the simulation.

We have also calculated the value of Hopf invariant directly from the field configuration. Using the basic differential geometric result of  $H(h \circ \chi \equiv \vec{n}) = \deg \chi$ , we can even use our computational field variables. Since for any map  $f \in C^\infty(S^3, S^3)$ ,

$$\deg f = \frac{1}{2 \cdot 3! \pi^2} \int_{S^3} \epsilon_{abcd} f^a df^b \wedge df^c \wedge df^d, \quad (36)$$

we can compute the value of the Hopf invariant by numerical integration. The other method is a visual inspection of linking numbers of preimages.

## IV. RESULTS AND DISCUSSION

### A. Stability of topological structures

A necessary condition for any stable static localized structure is its stability against scaling. Let us assume, for now, that  $\rho \neq 0$  everywhere. The simple procedure of Derrick<sup>34</sup> then provides us with a necessary condition for the stability against scaling. Consider the behavior of the energy under scaling  $x \rightarrow \lambda x$ . For the FS model in 3D the volume element behaves like  $\lambda^3$  while in the integrand (13) the first term scales as  $\lambda^{-2}$  and the second one as  $\lambda^{-4}$ . In the energy integral the two terms then have opposite behavior and if each is positive definite, one cannot scale the energy to zero. Indeed, one can show<sup>35</sup> that in the FS model the energy is bounded from below by the Hopf charge:  $E > c|Q|^{3/4}$ . This has also been confirmed numerically<sup>10,11,12,13</sup>.

In the present model the stability hinges on the behavior of the first and last terms in Eq. (18). The scaling properties of these two terms are opposite and thus, as long as they are both non-zero, the system is stable. The last term, however, equals the term  $\vec{B}^2$  in Eq. (1) and could, in principle, vanish. Indeed, if the  $\vec{C}$  field obtains the value

$$\epsilon_{ijk} \partial_j C_k = -\epsilon_{ijk} \vec{n} \cdot \partial_j \vec{n} \times \partial_k \vec{n}, \quad (37)$$

then the last term vanishes and the system is no longer stable under scaling. This is possible, since  $\vec{C}$  contains  $\vec{A}$ , which is in principle free.

Another possibility for topology breakdown is if  $\rho$  vanishes, even locally. This means  $\Psi_i = 0$  and we have no longer either of the superconducting phases but instead

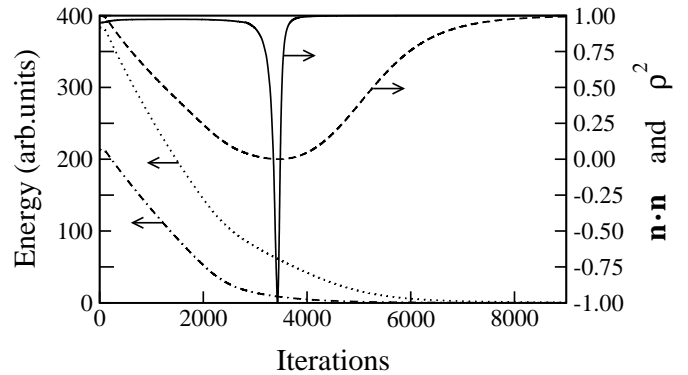


FIG. 1: Total energy (dotted line), energy of the  $\vec{B}^2$  term (dash-dotted line), the deviation of nearest-neighbor  $\vec{n}$  vectors ( $\vec{n} \cdot \vec{n} = 1$  indicates parallel and  $\vec{n} \cdot \vec{n} = -1$  antiparallel orientation), and the global minimum of  $\rho^2$  (dashed line) as a function of the number of iterations during the relaxation of the  $(m, n) = (1, 2)$  un-knot.

a normal phase. It also follows that both  $\chi_i$  and  $\vec{n}$  are then undetermined. From the point of view of  $\vec{n}$  this means that suddenly its domain is no longer the full  $S^3$ , but rather  $S^3$  with some points removed. The arguments about topological charge no longer hold and topology can break. This opens up the possibility of  $\vec{n}$  to change discontinuously in the domain where  $\rho = 0$ .

### B. Numerical simulations

We have investigated the two component GL model using un-knot initial states with non-vanishing topological charge  $Q = H(\vec{n})$ . The computational parameters of the system are shown in Table I.

| $H(\vec{n})$ | $m$ | $n$ | $N$                     | $a$      |
|--------------|-----|-----|-------------------------|----------|
| 1            | 1   | 1   | 120, 240, 480, 720, 960 | $10.0/N$ |
| 2            | 1   | 2   | 240, 480, 720, 960      | $10.0/N$ |
| 2            | 2   | 1   | 240, 480                | $10.0/N$ |
| 3            | 1   | 3   | 240                     | $10.0/N$ |
| 4            | 2   | 2   | 240                     | $9.0/N$  |

TABLE I: Initial configurations. Hopf invariant  $H(\vec{n}) = \deg \Phi$ , constants  $m$  and  $n$  from Eq. (30), number of grid points per axis  $N$ , and the lattice constant  $a$ .

In all simulations of Table I, with potentials  $V_0$  and  $V_1$ , the overall behavior is the same. As the iterations proceed the value of the field  $\rho^2$  drops down to 0 locally while at the same time the dot product  $\vec{n}(\vec{x}) \cdot \vec{n}(\vec{x} + \vec{\mu})$  goes to  $-1$ , see Fig. 1. (Since we use  $\Psi_i$  in the computation and not  $\vec{n}$ , the dot product is computed by writing it as a function of  $\Psi_i$  with the help of Eqs. (2), (3), and (11).) The fact that two neighboring  $\vec{n}$ -vectors are antiparallel implies that some part of the vortex configuration has shrunk to a size less than the lattice constant. We have also verified that these two events,  $\rho = 0$  and

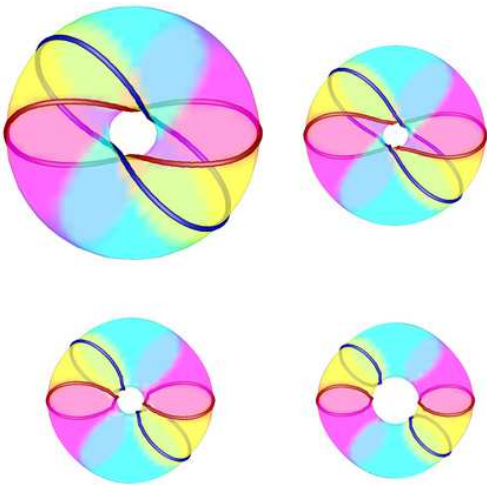


FIG. 2: Snapshots of the preimages in the relaxation of the  $(m, n) = (1, 2)$  un-knot. 0 (top left), 3300 (top right), 3500 (down left), and 3600 (down right). Topology breaks between iterations 3300 and 3500.

$\vec{n}(\vec{x}) \cdot \vec{n}(\vec{x} + \vec{\mu}) = -1$ , occur at the same place. Moreover, the topology breakdown can also be seen in the behavior of two distinct preimages (see Fig. 2), whose linking number gives the Hopf invariant of the system.

The behavior described above agrees with the scenarios discussed in the previous subsection: The quantity  $\rho^2$  going to zero indicates that a small volume of non-superconducting phase has formed in the system, and also that Eq. (11) is not well defined as discussed in Sec. II C. During the process where  $\rho^2 \rightarrow 0$  it also occurs that the energy of the  $B^2$  term in the Lagrangian approaches zero (see Fig. 1). As mentioned above this allows scaling and indeed both the radii of the torus decrease to zero (the smaller radius is defined by the isosurface of some specific value of  $n_3$ , say  $n_3 = 0$ ). For each system the total energy also decreases to zero monotonously.

We have also investigated whether the strength of the potential, i.e., the value of  $\lambda$  in Eq. (24), changes the behavior of the system. It turns out that the only effect that the parameter  $\lambda$  has on the system is the speed with which the minimum energy configuration is found: The stronger the potential, the slower the process, but nevertheless the topology always breaks down. Furthermore, increasing the number of lattice points cannot prevent the topology from breaking down either, because the scaling can go all the way to zero when  $\vec{B}^2 = 0$ . (This is in contrast with the FS model, where we had sometimes tightly knotted configurations whose structure was eventually resolved by increasing the lattice density.)

In the above the topology breakdown was associated with  $\rho \rightarrow 0$  locally. What if this is prevented by quantum effects, or in our classical field theory, by an effective potential  $V_{\text{eff}}$  in Eq. (27), or by keeping the value of  $\rho^2$

fixed to a constant non-zero value? Simulations for an un-knot, i.e., torus of a charge  $Q = 1$  in a lattice of  $240^3$  using the effective potential  $V_{\text{eff}}$  show that the global minimum of  $\rho^2$  decreases from its initial value as before, but now it drops down to a non-zero value after which it starts to increase again. Simultaneously the dot product  $\vec{n}(\vec{x}) \cdot \vec{n}(\vec{x} + \vec{\mu})$ , nevertheless, goes to  $-1$  locally. Increasing the lattice density to  $480^3$  or  $720^3$  grid points does not change the qualitative behavior of the system. The global minimum of  $\rho^2$  goes lower but still to a non-zero value and there are still antiparallel nearest-neighbor  $\vec{n}$  vectors in some region of the system. Even keeping the value of  $\rho^2$  fixed to a constant non-zero value does not change the behavior of the system.

In all cases the topology of the systems eventually breaks down by the same scenario: First, topological charge leaks from  $\vec{n}$  to  $\vec{C}$ , so that  $\vec{B} \rightarrow 0$ . After this the system can scale so that the region that contributes to the topological charge becomes smaller and smaller, eventually falling into the space between the lattice points. The form of the potential does not change this, because they do not change the scaling properties of the system.

The fact that the torus is transformed to a singular line can also be seen by monitoring the Hopf invariant in the system using Eq. (36) in the numerical integrations: The denser the grid, the sharper the drop of the charge from the original value to zero. We also checked this by plotting the Hopf invariant density (i.e. the value of the integrand in Eq. (36)) for some of these systems and found it to concentrate ever more tightly around the vortex core. This tells us that the region in which the charge is determined will eventually be in between the grid points used in the computation. Thus, it is not possible to prevent the breakdown of the topology making the grid even denser or e.g. with an adaptive grid.

It has to be noted that although the change of topology in its final stages is a consequence of the discreteness of the lattice, its fundamental cause, the fact that  $B^2$  goes to zero, is not. Thus, in a fully continuous analysis the conclusions would be the same.

## V. CONCLUSIONS

We have investigated numerically the two-component Ginzburg-Landau model using torus un-knots, with non-vanishing Hopf charge  $Q$ , as initial states; this brings a topological structure into the system. We have used different types of potentials depending on both of the order parameters  $\Psi_i$  ( $i = 1, 2$ ) of the system. In all the cases the system behaves similarly, i.e., the topological structure of the system eventually disappears, contrary to the case of the Faddeev-Skyrme model. The topological stability in the FS model is due to the fact that the kinetic and topological terms are non-vanishing and have an opposite behavior in the scaling. In the GL model, the term corresponding to the FS topological term is the magnetic field term which, however, can vanish, after which the

system becomes unstable against scaling. This is indeed what happens during energy minimization.

Thus, it seems that the two-component GL model does not support stable topological structures having a non-trivial conserved Hopf invariant, due to this scaling instability. How could this breakdown of topology be prevented? It seems that the only way is to either prevent the leakage of  $\vec{n}$  into  $\vec{C}$ , and therefore the vanishing of the  $B^2$  term, or by introducing other terms that scale as  $\partial^k$  with  $k > 3$ .

## Acknowledgments

We greatly acknowledge generous computing resources from the M-grid project, supported by the Academy of Finland, and from CSC – Scientific Computing Ltd., Espoo, Finland. This work has partly been supported by the Academy of Finland through its Center of Excellence program. One of us (J.J.) also wishes to thank Jenny and Antti Wihuri Foundation for a supporting grant.

- 
- \* Electronic address: juolja@utu.fi  
 † Electronic address: hietarin@utu.fi  
 ‡ Electronic address: pts@fyslab.hut.fi
- <sup>1</sup> J. R. Abo-Shaer, C. Raman, J. M. Vogels, and W. Ketterle, *Science* **292**, 476 (2001).
  - <sup>2</sup> P. Engels, I. Coddington, P. C. Haljan, V. Schweikhard, and E. A. Cornell, *Phys. Rev. Lett.* **90**, 170405 (2003).
  - <sup>3</sup> R. Carmi, E. Polturak, and G. Koren, *Phys. Rev. Lett.* **84**, 4966 (2000).
  - <sup>4</sup> R. Monaco, J. Mygind, M. Aaroe, R. J. Rivers, and V. P. Koshelets (2005), cond-mat/0503707.
  - <sup>5</sup> R. Monaco, J. Mygind, and R. J. Rivers, *Phys. Rev. Lett.* **89**, 080603 (2002).
  - <sup>6</sup> Ü. Parts, J. M. Karimäki, J. H. Koivuniemi, M. Krusius, V. M. H. Ruutu, E. V. Thuneberg, and G. E. Volovik, *Phys. Rev. Lett.* **75**, 3320 (1995).
  - <sup>7</sup> A. P. Finne, S. Boldarev, V. B. Eltsov, and M. Krusius, *Journal of Low Temperature Physics* **136**, 249 (2004).
  - <sup>8</sup> R. Ray and A. M. Srivastava, *Phys. Rev.* **D69**, 103525 (2004), hep-ph/0110165.
  - <sup>9</sup> L. D. Faddeev and A. J. Niemi, *Nature* **387**, 58 (1997), hep-th/9610193.
  - <sup>10</sup> R. A. Battye and P. M. Sutcliffe, *Phys. Rev. Lett.* **81**, 4798 (1998), hep-th/9808129.
  - <sup>11</sup> R. A. Battye and P. Sutcliffe, *Proc. Roy. Soc. Lond.* **A455**, 4305 (1999), hep-th/9811077.
  - <sup>12</sup> J. Hietarinta and P. Salo, *Phys. Lett.* **B451**, 60 (1999), hep-th/9811053.
  - <sup>13</sup> J. Hietarinta and P. Salo, *Phys. Rev.* **D62**, 081701 (2000).
  - <sup>14</sup> J. Hietarinta, J. Jäykkä, and P. Salo, *Phys. Lett.* **A321**, 324 (2004), cond-mat/0309499.
  - <sup>15</sup> C. Adam, J. Sanchez-Guillen, and A. Wereszczynski (2006), hep-th/0602008.
  - <sup>16</sup> J. P. Martikainen, A. Collin, and K. A. Suominen, *Phys. Rev. Lett.* **88**, 090404 (2002).
  - <sup>17</sup> M. Mackie, O. Dannenberg, J. Piilo, K.-A. Suominen, and J. Javanainen, *Phys. Rev.* **A69**, 053614 (2004), physics/0305057.
  - <sup>18</sup> J. Ruostekoski and Z. Dutton, *Phys. Rev.* **A72**, 063626 (2005), cond-mat/0507032.
  - <sup>19</sup> X.-J. Liu, H. Jing, X. Liu, and M.-L. Ge, *Eur. Phys. J. D* **37**, 261 (2006).
  - <sup>20</sup> E. Smorgrav, J. Smiseth, E. Babaev, and A. Sudbo, *Phys. Rev. Lett.* **94**, 096401 (2005), cond-mat/0411031.
  - <sup>21</sup> M. Donaire, T. W. B. Kibble, and A. Rajantie (2004), cond-mat/0409172.
  - <sup>22</sup> V. B. Eltsov, A. P. Finne, R. Hanninen, J. Kopu, M. Krusius, M. Tsubota, and E. V. Thuneberg, *Phys. Rev. Lett.* **96**, 215302 (2006).
  - <sup>23</sup> A. P. Finne, T. Araki, R. Blaauwgeers, V. B. Eltsov, N. B. Kopnin, M. Krusius, L. Skrbek, M. Tsubota, and G. E. Volovik, *Nature* **424**, 1022 (2003).
  - <sup>24</sup> E. Babaev, A. Sudbo, and N. W. Ashcroft, *Nature* **431**, 666 (2004), cond-mat/0410408.
  - <sup>25</sup> E. Babaev, *Phys. Rev.* **D70**, 043001 (2004), astro-ph/0211345.
  - <sup>26</sup> L. D. Faddeev, *Letters in Mathematical Physics* **1**, 289 (1976).
  - <sup>27</sup> E. Babaev, L. D. Faddeev, and A. J. Niemi, *Phys. Rev.* **B65**, 100512 (2002), cond-mat/0106152.
  - <sup>28</sup> In Ref.<sup>27</sup> there seems to be contradiction in the sign of  $j_k$  that affect some signs of other formulas as well.
  - <sup>29</sup> E. Babaev, private communication.
  - <sup>30</sup> L. D. Faddeev and A. J. Niemi, *Phys. Rev. Lett.* **85**, 3416 (2000), physics/0003083.
  - <sup>31</sup> H. Aratyn, L. A. Ferreira, and A. H. Zimerman, *Phys. Rev. Lett.* **83**, 1723 (1999), hep-th/9905079.
  - <sup>32</sup> K. G. Wilson, *Phys. Rev.* **D10**, 2445 (1974).
  - <sup>33</sup> P. H. Damgaard and U. M. Heller, *Phys. Rev. Lett.* **60**, 1246 (1988).
  - <sup>34</sup> G. H. Derrick, *J. Math. Phys.* **5**, 1252 (1964).
  - <sup>35</sup> A. F. Vakulenko and L. V. Kapitanskii, *Sov.Phys.Dokl.* **24**, 433 (1979).